

VIP

## Analytical Applications of Enzymatic Growth of Quantum Dots

Laura Saa, Ana Virel, Jose Sanchez-Lopez, and Valery Pavlov\*[a]

**Abstract:** We have developed an analytical assay to detect the enzymatic activity of acetylcholine esterase and alkaline phosphatase based on the generation of quantum dots by enzymatic products. Acetylcholine esterase converts acetylthiocholine into thiocholine. The latter enhances the rate of decomposition of sodium thiosulfate into H<sub>2</sub>S, which in the presence of cadmium sul-

phate yields CdS quantum dots showing a time dependent exponential growth, typical of autocatalytic processes. This assay was also applied to detect acetylcholine esterase inhibitors. Alkaline

phosphatase hydrolyzes thiophosphate and yields H<sub>2</sub>S, which instantly reacts with Cd<sup>2+</sup> to give CdS quantum dots. The formation of CdS quantum dots in both reactions was followed by fluorescence spectroscopy and showed dependence on the concentration of enzyme and substrate.

**Keywords:** emission spectroscopy • enzyme catalysis • quantum dots • semiconductors

## Introduction

Metallic and semiconductor nanoparticles are extensively employed in bioanalytical chemistry.<sup>[1,2]</sup> They demonstrate variation in surface plasmon resonance upon size or shape modifications leading to a change in the absorption spectra.<sup>[3]</sup> Inorganic semiconductor nanoparticles can be photoexcited to generate electron/hole couples, which recombine to yield fluorescent emission of light. The wavelength of emitted light depends on the nature and size of the semiconductor nanoparticles<sup>[4]</sup> and their emission properties are a consequence of quantum effects, hence they are frequently called quantum dots (QDs) in the literature. The most important advantages of QDs over organic fluorophores are higher brightness, reduced photobleaching and longer lifetimes.<sup>[5]</sup> QDs have been generally used as fluorescent labels in biosensing, especially in assays based on detection of analytes by affinity binding. For example, probe antibodies have been immobilized on a solid substrate, incubated with the analyte, and then, the antibodies tethered to QDs were added to detect the captured analyte.<sup>[6]</sup> Labeling of antibod-

ies with QDs with a range of sizes having different emission spectra allowed simultaneous fluorometric assays of a number of toxins in one sample.<sup>[7]</sup> QDs were also used as energy-transfer donors in assays based on fluorescence resonance energy transfer (FRET).<sup>[8,9]</sup> Some assays based on FRET have been reported in which fluorescent nanoparticles were modified with recognition elements for sugars<sup>[8]</sup> and explosives.<sup>[9]</sup> Cleavage of quenching acceptor molecules from the surface of QDs, tethered to them through degradable linkers, has been employed for the analysis of enzymatic activity of proteases.<sup>[10]</sup>

Enzymes are key components in bioanalytical assays. The most common enzyme-based biosensing strategies produce an optically or electrochemically readable signal for the detection of analytes, antigen–antibody interactions or microbial growth.<sup>[11,12]</sup> Bioanalytical assays based on enzymatic generation of nanoparticles are not very common. All reported assays are limited to biochemical growth of nonfluorescent metal nanoparticles. For instance, NADH generated by alcohol dehydrogenase, can reduce AuCl<sup>4-</sup> anions and grow spherical<sup>[13]</sup> and tripodal gold nanoparticles.<sup>[14]</sup> Copper was deposited on gold seed particles by reduction of Cu<sup>2+</sup> cations with NADH.<sup>[15]</sup> These reactions were used for the optical detection of ethanol. Production of gold nanoparticles by glucose oxidase mediated with a complex of osmium, Os-bis(bipyridine)-4-picolinic acid, was also reported.<sup>[16]</sup> The main drawback of the systems based on the enzymatic generation of metallic nanoparticles is that only UV/Vis spectroscopy can be utilized for the optical reading of a signal. A bioanalytical enzymatic system producing fluorescent

[a] Dr. L. Saa, Dr. A. Virel, J. Sanchez-Lopez, Dr. V. Pavlov  
Biofunctional Nanomaterials, CIC biomaGUNE  
Parque Tecnológico de San Sebastian, Paseo Miramon 182  
20009 San Sebastian (Spain)  
Fax: (+34) 943005314  
E-mail: vpavlov@cicbiomagune.es

Supporting information for this article is available on the WWW under <http://dx.doi.org/10.1002/chem.200903373>.

nanoparticles could employ a much more sensitive technique, such as fluorescence spectroscopy.

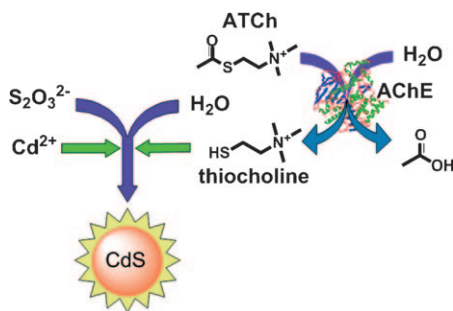
Here, we report two examples of enzymatic growth of CdS QDs and their analytical applications. We demonstrate that the reaction products of the two enzymes, acetylcholine esterase (AChE) and alkaline phosphatase (ALP), are able to catalyze the production of fluorescent nanoparticles and, as a result, enzymatic activity can be measured by fluorescence spectroscopy.

## Results and Discussion

Our first example of enzymatic generation of QDs with analytical applications is the reaction catalyzed by AChE, an enzyme that participates in the termination of the synaptic transmission by breaking down acetylcholine at cholinergic synapses.<sup>[17]</sup> Inhibitors of AChE, such as nerve gases and pesticides, are able to block enzymatic decomposition of acetylcholine, causing fatal consequences.<sup>[18]</sup> AChE can also hydrolyze the alternative artificial substrate acetylthiocholine (ATCh) and yield the thiol-containing compound thiocholine and acetic acid. Our method consists of the synthesis of CdS QDs in the presence of thiosulfate, cadmium sulfate and thiocholine. It is known that anions of thiosulfate,  $S_2O_3^{2-}$  are reduced to  $H_2S$ , which in the presence of  $Cd^{2+}$  cations form nanocrystals of CdS. The reactions can be summarized as follows:<sup>[19]</sup>



The rate of the first reaction is slow, but thiol-containing organic compounds promote the decomposition of  $S_2O_3^{2-}$  to  $H_2S$ .<sup>[20,21]</sup> We have used the enzymatically produced thiocholine as a thiol to trigger the formation of CdS QDs. The operating principle of our system is depicted in Scheme 1. When AChE hydrolyzes ATCh yields thiocholine, which in turn catalyzes the hydrolysis of  $S_2O_3^{2-}$ . The resulting  $H_2S$  reacts with  $Cd^{2+}$  cations to give fluorescent CdS nanocrystals.



Scheme 1. Enzymatic generation of CdS QDs for the detection of AChE activity.

Figure 1A shows the UV/Vis and emission spectra (solid and dashed lines, respectively) of the CdS nanoparticles produced by enzymatic hydrolysis of ATCh. From the UV/Vis spectrum we observe increased absorption below 480 nm, and a shoulder at about 380 nm. The presence of this shoulder is explained by  $1S_h-1S_e$  excitonic transition<sup>[22]</sup> characteristic of nanoparticles with a diameter of  $\sim 2-3$  nm, according to the work of Peng et al.<sup>[23]</sup> From the emission spectrum of enzymatically generated CdS QDs we observe a maximum at 600 nm and a lower peak at 440 nm, which arises from excitonic emission of CdS nanoparticles.<sup>[24]</sup> The size of CdS nanoparticles was determined by high resolution transmission electron microscopy (TEM). TEM analysis confirmed the data obtained from UV/Vis and fluorescence spectra (Figure 1B). The nanoparticles appear as very homogeneously sized spheroidal nanocrystallites, and the diameter was calculated to be between 2–3 nm. The presence of cadmium and sulfur in the sample was confirmed by energy dispersive X-ray spectroscopy (EDXS; data not shown).

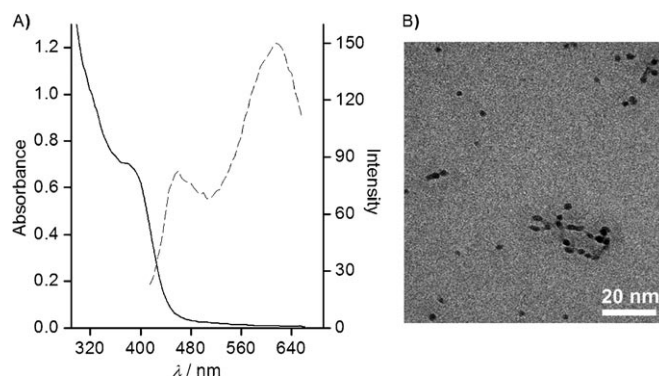


Figure 1. A) Absorption (—) and emission (---) spectra of the CdS QDs formed in the presence of ATCh (16 mM), AChE (25  $U mL^{-1}$ ), sodium thiosulfate (0.3 M) and  $CdSO_4$  (1 mM). B) TEM image of the CdS QDs formed in the presence of ATCh (16 mM), AChE (10  $U mL^{-1}$ ), sodium thiosulfate (0.3 M) and  $CdSO_4$  (1 mM). The diameter of the QDs was calculated to be between 2 and 3 nm.

The formation of the enzymatically produced CdS QDs was followed by fluorescence spectroscopy. We first investigated the effect of AChE concentration on the formation of the CdS QDs. Figure 2 outlines the evolution of the fluorescence intensities in the presence of a fixed concentration of ATCh and varying concentrations of AChE. We observed that increasing amounts of AChE were correlated with a decrease in the time of generation of the CdS QDs. The increase in fluorescence intensity even in the absence of AChE (curve a) is caused by spontaneous hydrolysis of ATCh to thiocholine. The obtained curves showed an exponential growth of fluorescence, which was especially apparent at low concentrations of AChE, suggesting that the process of formation of QDs induced by thiocholine is autocatalytic. It is well known that during the growth of spherical solid nanoparticles newly formed nanocrystals can detach from the surface of growing particles and serve as centers of

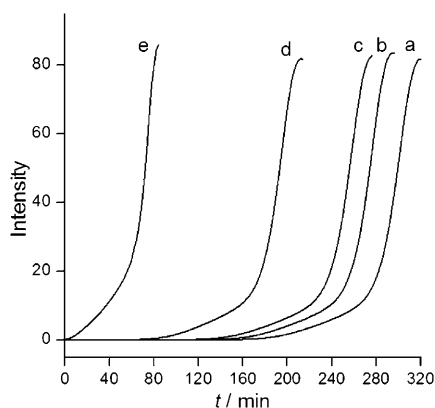


Figure 2. Evolution of the fluorescence intensity of the CdS QDs formed in the presence of ATCh (10 mM) and different concentrations of AChE: a) 0  $\mu\text{M mL}^{-1}$ ; b) 25  $\mu\text{M mL}^{-1}$ ; c) 50  $\mu\text{M mL}^{-1}$ ; d) 100  $\mu\text{M mL}^{-1}$ ; and e) 250  $\mu\text{M mL}^{-1}$ . In all experiments, the system included sodium thiosulfate (0.3 M) and  $\text{CdSO}_4$  (1 mM).

nucleation for deposition of more material,<sup>[25,26]</sup> indicating that the kinetics of this process has an autocatalytic behavior. The traditional version of calibration curves based on the intensity of readout signal measured at a fixed time is not suitable for representation of autocatalytic analytical systems. The time and stage of maximum autocatalytic rate depends on the concentration of an analyte. The use of the time of maximum rate instead of fixed time measurements of fluorescence intensities would allow us to obtain more accurate calibration plots corresponding to each concentration of AChE and ATCh.

To analyze the effect of AChE and ATCh on CdS QD formation rate, we plotted the first derivative of fluorescence intensity with respect to time ( $dI/dt$ ) versus time (Figure S1 and S2 in Supporting Information). The peaks on the curves reveal the exact time of maximum autocatalytic rate corresponding to each concentration of AChE and ATCh. We plotted the time of maximum autocatalytic rate versus the concentration of ATCh and AChE (Figure 3 A and B) and

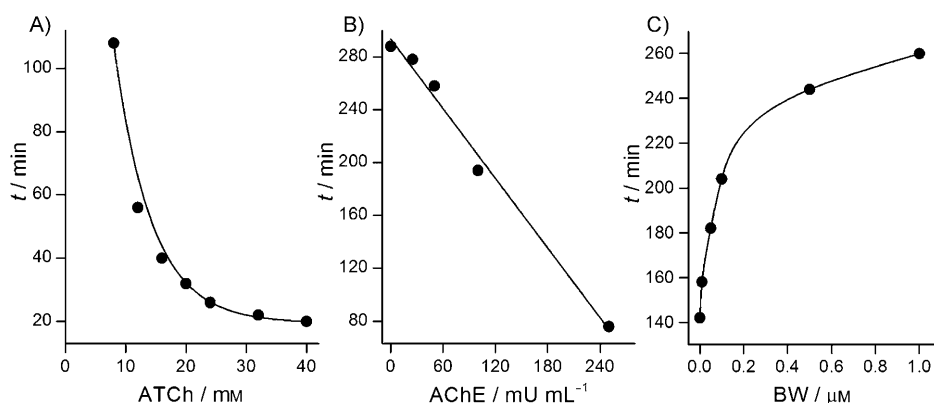


Figure 3. Time of maximum catalytic rate for the generation of CdS QDs formed in the presence of: A) AChE (25  $\mu\text{M mL}^{-1}$ ) and different concentrations of ATCh; B) ATCh (10 mM) and different concentrations of AChE; C) AChE (0.1  $\mu\text{M mL}^{-1}$ ), ATCh (10 mM) and different concentrations of BW284c51 (BW). In all experiments, the system included sodium thiosulfate (0.3 M) and  $\text{CdSO}_4$  (1 mM).

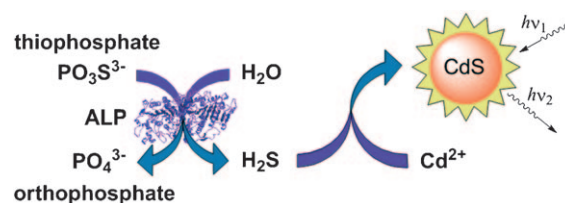
observed that increasing amounts of ATCh or AChE were correlated with a shortening of the time of CdS QD formation. This clearly indicated that when the concentration of either AChE or ATCh is increased, the concentration of thiocholine also increases. As the decomposition of thiosulfate is promoted in the presence of thiocholine, a rise in the amount of thiocholine in our system causes an increase in the rate of release of  $\text{H}_2\text{S}$ , triggering the formation of CdS QDs. It should be noted that no growth of fluorescence occurred in the absence of ATCh. This observation confirms that the spontaneous hydrolysis of ATCh is the cause of nonspecific signal in the present system. To confirm the catalytic effect of thiocholine in our system, control experiments were performed using different amounts of the water-soluble organic thiols, thioglycerol and  $\beta$ -mercaptoethanol, instead of thiocholine. The obtained curves showed similar exponential development of the evolved fluorescence intensities (Figure S3 in Supporting Information).

In order to provide more evidence that specifically the enzymatic activity of AChE induced the formation of CdS QDs, we employed the cholinesterase inhibitor 1,5-bis(4-allyldimethylammoniumphenyl)pentan-3-one dibromide (BW284c51), which has a mechanism of toxicity similar to organophosphorous nerve agents and is frequently utilized as an analogue of nerve gases.<sup>[27,28]</sup> This inhibitor has a high selectivity for AChE and competes with the substrate for binding to the active site of the enzyme. The effect of various concentrations of BW284c51 on the evolution of fluorescence in our system was studied (Figure S4 in the Supporting Information). Figure 3 C shows the time of maximum autocatalytic rate of the generation of CdS QDs formed in the presence of AChE preincubated with different amounts of BW284c51. We observed from this representation that increasing amounts of the inhibitor were correlated with an increase in the time of generation of QDs. This indicates that the higher the amount of the inhibitor, the lower is the amount of AChE available to generate thiocholine and promote the growth of the CdS QDs.

In addition, we developed a second analytical enzymatic system in which generation of CdS QDs was linked to the presence of ALP, an enzyme that removes phosphate groups from biomolecules, such as alkaloids, proteins and nucleotides. ALP finds wide application in bioanalysis as a label in enzyme linked immunosorbent assays (ELISA), Southern, Western and Northern blotting and dot/slot blots. Another important application of ALP is the monitoring of pasteurization in cows' milk—well-pasteurized milk should not demonstrate any phosphatase activi-

ty due to enzyme deactivation at elevated temperature.<sup>[29]</sup> Measurement of ALP activity in human blood serum is also used for the diagnostics of viral acute and chronic hepatitis and cirrhosis. The ALP activity is tested by chromogenic substrates: *p*-nitrophenyl phosphate,<sup>[30]</sup> 5-bromo-4-chloro-3-indolyl phosphate,<sup>[31,32]</sup> and 1-naphthyl phosphate disodium salt.<sup>[33]</sup> Fluorogenic substrates based on 4-methylumbelliferone have also been employed in the activity assay of ALP.<sup>[34]</sup> The disadvantages of these methods include high costs, special storage conditions and maximum fluorescence of the reaction product at alkaline pH.<sup>[35]</sup>

Here, we offer an alternative concept for measurements of ALP activity, based on the synthesis of CdS QDs in the presence of ALP, thiophosphate and Cd(NO<sub>3</sub>)<sub>2</sub>. The mechanism of this system is depicted in Scheme 2 and can be described as follows: in the presence of ALP, thiophosphate is hydrolyzed to orthophosphate and H<sub>2</sub>S.<sup>[36]</sup> The latter reacts immediately with cadmium cations and gives CdS QDs. When these CdS QDs are excited at 360 nm a strong fluorescence signal is observed. Figure 4A (curve a) shows the



Scheme 2. Enzymatic generation of CdS QDs for the detection of ALP activity.

thiophosphate result in an increase in the fluorescence signal. This clearly indicates that thiophosphate is hydrolyzed by ALP to orthophosphate, which reacts with Cd<sup>2+</sup> to form fluorescent CdS QDs. We also studied the influence of ALP concentration on the resulting fluorescence using 75 μM as the optimal concentration of thiophosphate (Figure 5C and D). From the calibration plot we also observe that increasing amounts of ALP lead to an increase in the fluorescence signal, since ALP is the catalyst of the reaction. Using an S/N=3 we calculated a detection limit for ALP of 8 ng mL<sup>-1</sup>. We performed the same enzymatic assay using the chromogenic substrate *p*-nitrophenyl phosphate and obtained a detection limit of 35 ng mL<sup>-1</sup> (data not shown), signifying that our method is four-times more sensitive than

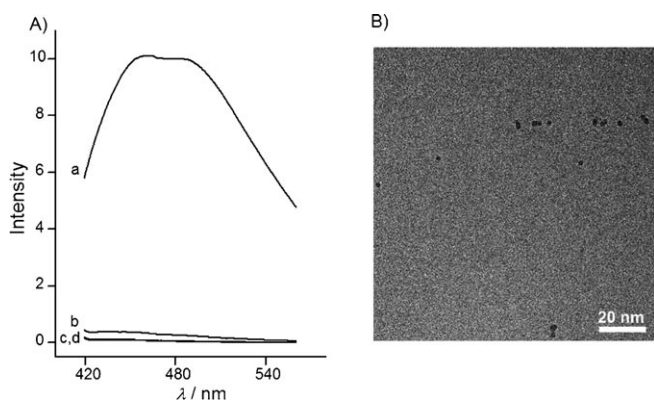


Figure 4. A) Emission spectra of the CdS QDs formed in the presence of: a) ALP (228 ng mL<sup>-1</sup>), sodium thiophosphate (75 μM) and Cd(NO<sub>3</sub>)<sub>2</sub> (2.5 mM); b) sodium thiophosphate (75 μM) and Cd(NO<sub>3</sub>)<sub>2</sub> (2.5 mM); c) ALP (228 ng mL<sup>-1</sup>) and Cd(NO<sub>3</sub>)<sub>2</sub> (2.5 mM); d) ALP (228 ng mL<sup>-1</sup>) and sodium thiophosphate (75 μM). B) TEM image of the CdS QDs formed in the presence of ALP (228 ng mL<sup>-1</sup>), sodium thiophosphate (75 μM) and Cd(NO<sub>3</sub>)<sub>2</sub> (2.5 mM). The diameter of the QDs was calculated to be between 1 and 3 nm.

emission spectrum of the system composed of ALP, sodium thiophosphate and Cd(NO<sub>3</sub>)<sub>2</sub>. This emission spectrum is characterized by a broad peak with a maximum emission at about 445 nm. In contrast, when one of the essential components is withdrawn from the system no detectable growth in fluorescence is observed (curves b, c, d), confirming that the fluorescence developed in the system can be attributed to the formation of QDs. Figure 4B shows TEM images of CdS nanoparticles generated in the system containing all the necessary components. The formed nanoparticles have a spherical shape with a median diameter of 1.9 nm.

The effect of the concentration of thiophosphate on the developed fluorescence is presented in Figure 5A and B. From the spectra we can observe that increasing amounts of

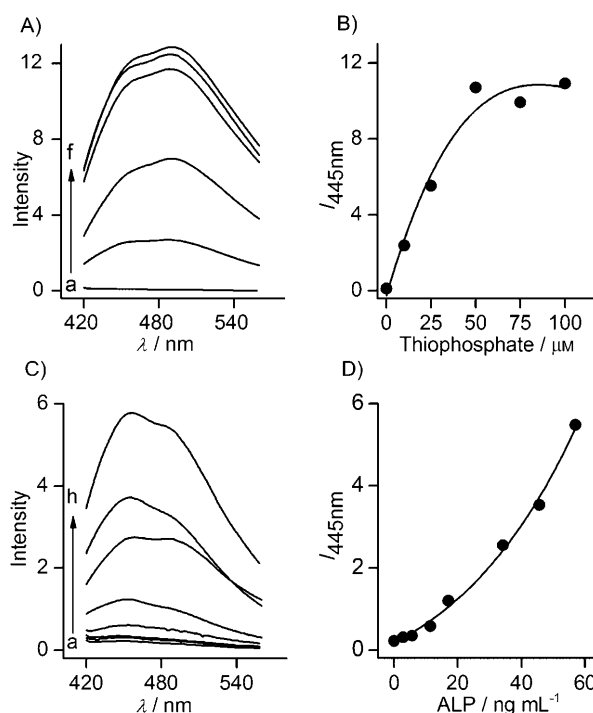


Figure 5. A) Emission spectra in the system containing ALP (228 ng mL<sup>-1</sup>), Cd(NO<sub>3</sub>)<sub>2</sub> (2.5 mM) and various concentrations of sodium thiophosphate: a) 0 μM; b) 10 μM; c) 25 μM; d) 50 μM; e) 75 μM; and f) 100 μM. B) Calibration curve of sodium thiophosphate at λ=445 nm. C) Emission spectra in the system containing sodium thiophosphate (75 μM), Cd(NO<sub>3</sub>)<sub>2</sub> (2.5 mM) and various concentrations of ALP: a) 0 ng mL<sup>-1</sup>; b) 2.85 ng mL<sup>-1</sup>; c) 5.7 ng mL<sup>-1</sup>; d) 11.4 ng mL<sup>-1</sup>; e) 17.1 ng mL<sup>-1</sup>; f) 34.2 ng mL<sup>-1</sup>; g) 45.6 ng mL<sup>-1</sup>; and h) 57 ng mL<sup>-1</sup>. D) Calibration curve of ALP at λ=445 nm.

the commercial assay. We believe that our activity assay based on the enzymatic formation of fluorescent CdS QDs can find broad application for measurement of ALP in a large number of bioanalytical assays, such as ELISA, or detection of low levels of ALP in whole blood without the separation of the serum, which is compulsory in case of chromogenic substrates. The present activity assay can also be employed in monitoring the quality of milk pasteurization. Our method can significantly reduce time and costs related with these important tests.

## Conclusion

In summary, the present study has introduced a new analytical approach in which the enzymatic generation of QDs can be applied to the detection of enzymatic activities. Using the products of the reactions catalyzed by AChE and ALP, we have been able to produce CdS QDs that show a characteristic fluorescence, dependent on the concentration of enzyme or substrate. The formation of CdS QDs can be measured by fluorescence spectroscopy and represents an alternative to other analytical methods.

## Experimental Section

**Materials:** Acetylcholine esterase (from electric eel), alkaline phosphatase (from *Escherichia coli*), acetylthiocholine chloride, sodium thiosulfate ( $\text{Na}_2\text{S}_2\text{O}_3$ ), cadmium nitrate ( $\text{Cd}(\text{NO}_3)_2$ ), cadmium sulfate ( $\text{CdSO}_4$ ), 1,5-bis(4-allyldimethylammoniumphenyl)pentan-3-one dibromide (BW284c51) and sodium thiophosphate ( $\text{Na}_3\text{SPO}_3$ ) were obtained from Sigma-Aldrich and used as supplied. The absorbance and fluorescence spectra were recorded in a spectrophotometer ND-1000 (Nanodrop Technologies) and in a FluoroLog (Horiba Jobin Yvon) fluorometer, respectively. The time evolution of the fluorescence was monitored in a Plate Reader GeniosPro (Tecan).

**Acetylcholine esterase assay:** Various amounts of acetylthiocholine chloride were incubated with different amounts of acetylcholine esterase in HEPES buffer (0.01 M, pH 8.0) at 37°C for 90 min. This mixture (100  $\mu\text{L}$ ) was added to a solution (100  $\mu\text{L}$ ) consisting of  $\text{CdSO}_4$  (2 mM) and sodium thiosulfate (0.6 M) in water. The fluorescence of the resulting solutions was recorded every 3 min at  $\lambda_{\text{exc}} = 340$  nm and  $\lambda_{\text{em}} = 612$  nm.

**Inhibition of acetylcholine esterase by 1,5-bis(4-allyldimethylammoniumphenyl)pentan-3-one dibromide (BW284c51):** Acetylcholine esterase (0.2  $\text{U mL}^{-1}$ ) was incubated with different concentrations of BW284c51 in HEPES buffer (0.01 M, pH 8.0) at room temperature for 2 h. Next, this mixture (50  $\mu\text{L}$ ) was added to a solution (50  $\mu\text{L}$ ) containing acetylthiocholine chloride (20 mM) in HEPES buffer (0.01 M, pH 8.0) and incubated at 37°C for 90 min. After that, the mixture was added to a solution (100  $\mu\text{L}$ ) consisting of  $\text{CdSO}_4$  (2 mM) and sodium thiosulfate (0.6 M) in water. The fluorescence of the resulting suspensions was measured every 3 min at  $\lambda_{\text{exc}} = 340$  nm and  $\lambda_{\text{em}} = 612$  nm.

**Alkaline phosphatase assay:** Various amounts of sodium thiophosphate were incubated with different amounts of alkaline phosphatase in Tris-HCl buffer (0.05 M, pH 8.8) containing  $\text{MgCl}_2$  (1 mM) at 37°C for 90 min. After that,  $\text{Cd}(\text{NO}_3)_2$  (5  $\mu\text{L}$ , 0.5 M) was added to this mixture (995  $\mu\text{L}$ ). The emission spectra of the resulting suspensions were recorded after 30 min at  $\lambda_{\text{exc}} = 360$  nm.

## Acknowledgements

This work was supported by the Department of Industry of the Basque Government (ETORTEK, 2006–2008) and the Spanish Ministry of Science and Innovation (project BIO2008-04856). V.P. acknowledges the contract Ramon y Cajal from the Spanish Ministry of Science and Innovation. The contribution of the Electron Microscopy study by Marco Möller (CIC biomaGUNE) and David Gil (CIC bioGUNE) is gratefully acknowledged.

- [1] C. M. Niemeyer, *Angew. Chem.* **2001**, *113*, 4254–4287; *Angew. Chem. Int. Ed.* **2001**, *40*, 4128–4158.
- [2] E. Katz, I. Willner, *Angew. Chem.* **2004**, *116*, 6166–6235; *Angew. Chem. Int. Ed.* **2004**, *43*, 6042–6108.
- [3] L. M. Liz-Marzán, *Mater. Today* **2004**, *7*, 26–31.
- [4] W. J. Parak, L. Manna, F. C. Simmel, D. Gerion, P. Alivisatos in *Nanoparticles: From Theory to Application* (Ed.: S. Günter), Wiley-VCH, Weinheim, **2004**, pp. 4–49.
- [5] C.-A. J. Lin, T. Liedl, R. A. Sperling, M. T. Fernandez-Arguelles, J. M. Costa-Fernandez, R. Pereiro, A. Sanz-Medel, W. H. Chang, W. J. Parak, *J. Mater. Chem.* **2007**, *17*, 1343–1346.
- [6] B. Sun, W. Xie, G. Yi, D. Chen, Y. Zhou, J. Cheng, *J. Immunol. Methods* **2001**, *249*, 85–89.
- [7] E. R. Goldman, A. R. Clapp, G. P. Anderson, H. T. Uyeda, J. M. Mauro, I. L. Medintz, H. Mattoussi, *Anal. Chem.* **2004**, *76*, 684–688.
- [8] E. R. Goldman, I. L. Medintz, J. L. Whitley, A. Hayhurst, A. R. Clapp, H. T. Uyeda, J. R. Deschamps, M. E. Lassman, H. Mattoussi, *J. Am. Chem. Soc.* **2005**, *127*, 6744–6751.
- [9] I. L. Medintz, A. R. Clapp, H. Mattoussi, E. R. Goldman, B. Fisher, J. M. Mauro, *Nat. Mater.* **2003**, *2*, 630–638.
- [10] I. L. Medintz, A. R. Clapp, F. M. Brunel, T. Tiefenbrunn, H. Tetsuo Uyeda, E. L. Chang, J. R. Deschamps, P. E. Dawson, H. Mattoussi, *Nat. Mater.* **2006**, *5*, 581–589.
- [11] M. Mehrvar, M. Abdi, *Anal. Sci.* **2004**, *20*, 1113–1126.
- [12] J. L. Reymond, V. S. Fluxa, N. Maillard, *Chem. Commun.* **2009**, 34–46.
- [13] Y. Xiao, V. Pavlov, S. Levine, T. Niazov, G. Markovitch, I. Willner, *Angew. Chem.* **2004**, *116*, 4619–4622; *Angew. Chem. Int. Ed.* **2004**, *43*, 4519–4522.
- [14] Y. Xiao, B. Shlyahovsky, I. Popov, V. Pavlov, I. Willner, *Langmuir* **2005**, *21*, 5659–5662.
- [15] B. Shlyahovsky, E. Katz, Y. Xiao, V. Pavlov, I. Willner, *Small* **2005**, *1*, 213–216.
- [16] Y. Xiao, V. Pavlov, B. Shlyahovsky, I. Willner, *Chem. Eur. J.* **2005**, *11*, 2698–2704.
- [17] G. Zimmerman, H. Soreq, *Cell Tissue Res.* **2006**, *326*, 655–669.
- [18] B. E. Mileson, J. E. Chambers, W. L. Chen, W. Dettbarn, M. Ehrlich, A. T. Eldefrawi, D. W. Gaylor, K. Hamernik, E. Hodgson, A. G. Karczmar, S. Padilla, C. N. Pope, R. J. Richardson, D. R. Saunders, L. P. Sheets, L. G. Sultatos, K. B. Wallace, *Toxicol. Sci.* **1998**, *41*, 8–20.
- [19] V. Swayambunathan, D. Hayes, K. H. Schmidt, Y. X. Liao, D. Meisel, *J. Am. Chem. Soc.* **1990**, *112*, 3831–3837.
- [20] Y. J. Yang, J. W. Xiang, *Appl. Phys. A* **2005**, *81*, 1351–1353.
- [21] Y. J. Yang, *Colloids Surf. A* **2006**, *276*, 192–196.
- [22] H. Matsumoto, T. Sakata, H. Mori, H. Yoneyama, *J. Phys. Chem.* **1996**, *100*, 13781–13785.
- [23] W. W. Yu, L. Qu, W. Guo, X. Peng, *Chem. Mater.* **2003**, *15*, 2854–2860.
- [24] P. Mandal, S. S. Talwar, S. S. Major, R. S. Srinivasa, *J. Chem. Phys.* **2008**, *128*, 114703.
- [25] R. Möller, A. Csaki, J. M. Kohler, W. Fritzsche, *Langmuir* **2001**, *17*, 5426–5430.
- [26] M. Zayats, R. Baron, I. Popov, I. Willner, *Nano Lett.* **2005**, *5*, 21–25.
- [27] L. Austin, W. K. Berry, *Biochem. J.* **1953**, *54*, 695–700.
- [28] A. Vale, S. Bradberry, P. Rice, T. C. Marrs, *Medicine* **2003**, *31*, 26–29.
- [29] R. Aschaffenburg, J. E. C. Mullen, *J. Dairy Res.* **1949**, *16*, 58–67.

- [30] O. H. Lowry in *Methods Enzymol.*, Vol. 4, Academic Press, New York, **1957**, pp. 366–381.
- [31] J. McGadey, *Histochemie* **1970**, 23, 180–184.
- [32] J. P. Horwitz, J. Chua, M. Noel, J. T. Donatti, J. Freisler, *J. Med. Chem.* **1966**, 9, 447–447.
- [33] T. W. Reid, I. B. Wilson in *The Enzymes*, Vol. IV, 3rd ed. (Ed.: P. D. Boyer), Academic Press, New York, **1971**, pp. 373–415.
- [34] H. N. Fernley, P. G. Walker, *Biochem. J.* **1965**, 97, 95–103.
- [35] K. R. Gee, W. C. Sun, M. K. Bhalgat, R. H. Upson, D. H. Klaubert, K. A. Latham, R. P. Haugland, *Anal. Biochem.* **1999**, 273, 41–48.
- [36] J. F. Chlebowski, J. E. Coleman, *J. Biol. Chem.* **1974**, 249, 7192–7202.

Received: December 9, 2009  
Published online: April 29, 2010